Gamow-Teller transitions to ^{32}P studied through the ^{32}S$(d,^2$He$)$ reaction at $E_d=170$ MeV

E. W. Grewe,[1] C. Bäumer,[1] A. M. van den Berg,[2] N. Blasi,[3] B. Davids,[2,*] D. De Frenne,[4] D. Frekers,[1] P. Haefner,[1] M. N. Harakeh,[2] M. Huynyadi,[2,†] E. Jacobs,[4] B. Junk,[1] A. Korff,[1] A. Negret,[4,‡] P. von Neumann-Cosel,[5] L. Popescu,[4,‡] S. Rakers,[1] and H. J. Wörtche[2]

[1]*Institut für Kernphysik, Westfälische Wilhelms-Universität Münster, D-48149 Münster, Germany*

[2]*Kernfysisch Verneller Instituut, Rijksuniversiteit Groningen, NL-9747 AA Groningen, The Netherlands*

[3]*INFN, Sezione di Milano, I-20133 Milano, Italy*

[4]*Vakgroep Subatomaire en Stralingsfysica, Universiteit Gent, B-9000 Gent, Belgium*

[5]*Institut für Kernphysik, Techische Universität Darmstadt, D-64289 Darmstadt, Germany*

(Received 20 February 2004; published 28 June 2004)

The ^{32}S$(d,^2$He$)^{32}$P charge-exchange reaction has been studied at forward angles and at an incident energy of $E_d=170$ MeV. The two protons in the $^1S_0(pp)$ state (indicated as ^{2}He) were both momentum analyzed and detected by the same spectrometer and detector. High resolution ^{2}He spectra have been obtained allowing identification of many levels in the residual nucleus with high precision. The $(d,^2$He) reaction selectively excites spin-isospin-flip transitions, and at vanishing momentum transfer these are largely governed by the Gamow-Teller transition operator for the β^+ direction. In the case of the self-conjugate nucleus ^{32}S, the $(d,^2$He) probe is calibrated against the elementary (p,n) probe going into the mirror β^- direction. The deduced results are compared with those obtained from (p,p') and (e,e') reactions, which excite the same levels in the isospin multiplet. Angular distributions of cross sections for the $(d,^2$He) reaction are presented and compared with DWBA calculations. A level-by-level comparison with shell-model calculations using the USD interaction has been performed, and the structure of the *l*-forbidden ground state transition is discussed. From the comparison with (p,p'), (e,e'), and (p,n) data the isospin-analog $J^\pi=1^+$ levels in the triplet of the $A=32$ nuclei are deduced.

DOI: 10.1103/PhysRevC.69.064325 PACS number(s): 21.10.Hw, 23.40.Hc, 25.45.Kk, 27.30.+t

I. INTRODUCTION

The $(d,^2$He) charge-exchange reaction has recently been used as a viable alternative to the (n,p) reaction because energy resolutions of about 140 keV in the final nucleus could readily be achieved [1–4]. This resolution is to be compared with a typical 1.3 MeV resolution obtained in the pioneering TRIUMF experiments with the (n,p) reactions [5]. As (n,p)-type charge-exchange reactions at forward scattering angles probe the Gamow-Teller (GT) transition strength distributions for the β^+ direction in the nucleus, they can be of significant astrophysical importance for the understanding of supernova explosion dynamics and element formation [6,7]. However, when using charge-exchange probes other than the elementary (n,p)-type, compositeness becomes a rather significant shortcoming. Furthermore, if heavy-ion reactions like $(^{6,7}$Li$,^{6,7}$Be) [8] or $(^{12}$C$,^{12}$N) [9,10] at several hundred MeV per nucleon are used, resolution becomes an issue again, leaving presently only a narrow window for light ions, like for instance $(d,^2$He) but also $(t,^3$He) [11,12]. For $(d,^2$He) reactions, compositeness in the traditional sense may not be such an important issue, as the neutron in the incoming deuteron can safely be regarded as quasifree. Here, it is the outgoing two-proton system that complicates the reaction. Two aspects may summarize the situation:

(i) The incident deuteron is a rather pure $^3S_1$ $(T=0)$ state and the $(d,^2$He) reaction is therefore of isovector spin-flip type. Further, the limited acceptance of the spectrometer, which in turn limits the relative energy of the detected ^{2}He to $\varepsilon<1.0$ MeV, usually ensures that partial waves for the ^{2}He di-proton system other than $^1S_0$ do not play a significant role. This selectivity, however, is counterbalanced by the fact that, for the same reason, one cannot exhaust all of the total $^1S_0$ phase space and consequently the available GT strength.

(ii) At finite momentum transfers it remains unclear if the transferred momentum is being carried away by the ^{2}He system as a whole, or if it is unevenly transferred to its constituents, in which case the ^{2}He di-proton system may break apart. Some additional momentum dependence in the cross section beyond what one would expect from the elementary (n,p) reaction is thus expected.

Fortunately, the momentum dependence does not seem to be too significant, as has recently been shown when comparing GT strength parameters for the ground and excited states of ^{12}C and ^{24}Mg [1]. This finding is corroborated by the present analysis on ^{32}S. The limited phase-space acceptance of the $^1S_0$ *pp*-system, however, requires the introduction of an additional scaling parameter to relate the reaction strengths of $(d,^2$He) to (n,p). In order to evaluate this scaling parameter, which we assume to be mass and momentum independent, one can employ the isospin symmetry between (p,n) and (n,p) reactions on self-conjugate nuclei. However, one should be cognizant of the fact that this symmetry might

*Present address: TRIUMF, 4004 Wesbrook Mall, Vancouver, B.C., Canada.

†Present address: ATOMKI, Debrecan, Hungary.

‡Permanent address: NIPNE, Bucharest, Romania.

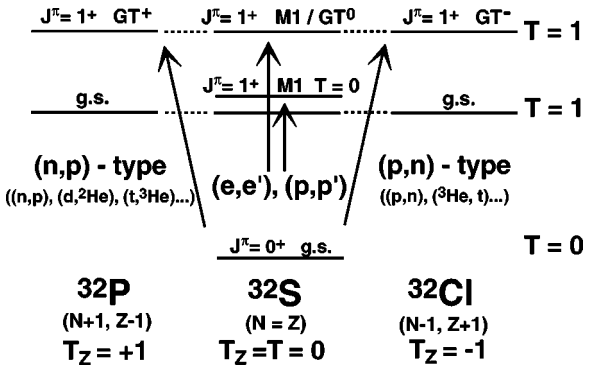

FIG. 1. Isospin of $J^\pi=1^+$ states excited from the ground state of ^{32}S with $T=0$ and $T_z=0$. Isobaric analog states are connected by dashed lines.

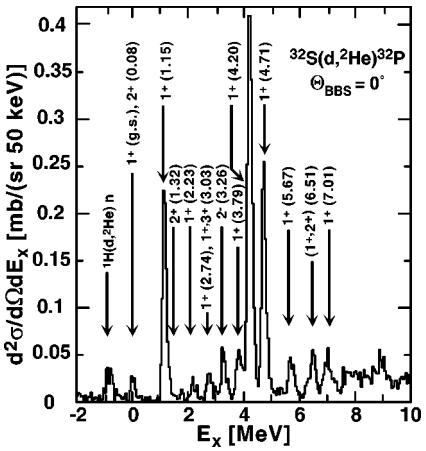

FIG. 2. Excitation energy spectrum of ^{32}P at $\Theta_{BBS}=0°$ showing the levels excited by the present $(d,^2\mathrm{He})$, reaction.

be broken at some level when comparing individual states [13,14].

Charge-exchange reactions in the β^- direction have been studied extensively through (p,n) [15–17] and more recently through $(^3\mathrm{He},t)$ reactions [18,19]. Also (p,p') and (e,e') reactions can be used, which, under appropriate kinematic conditions, will excite the $(T+1)$ isospin analog states in the target nucleus. Figure 1 summarizes the excitation modes of the 1^+ states with isospin $T=1$ starting from a $T=0$ ground state. In the present case of ^{32}S we have the fortuitous situation that high resolution data for each of these probes, i.e., (p,n), (p,p') and (e,e'), are available together with the respective strength parameters [15,20,21].

II. EXPERIMENT

The present experiment was performed at the KVI Groningen using the ESN detector [22–24], which consists of a focal-plane detection system with two vertical drift chambers and another tracking detector, which is a set of four multi-wire proportional chambers. The detector is located near the focal plane of the Big-Bite Spectrometer (BBS) [25]. A full account of how the $(d,^2\mathrm{He})$ experiments are performed and analyzed can be found in Ref. [3].

A beam of 170 MeV deuterons was delivered by the AGOR cyclotron. The spectrometer and the beam line were setup in dispersion-matched mode to ensure good momentum resolution [26].

The target consisted of natural sulphur pressed to an oval pellet of 8.8 mg/cm^2 thickness. This is equivalent to 8.4 mg/cm^2 of ^{32}S. The pellet, whose size was about 4 $\times$10 mm^2, was embedded into a carbon frame and covered on both sides with thin carbon foils each of about 0.1 mg/cm^2. We decided to use carbon as a target carrier material, as the Q-value of the $^{12}\mathrm{C}(d,^2\mathrm{He})^{12}\mathrm{B}$ reaction is -14.9 MeV, and the ^{12}B ground state peak would be found in the ^{32}P spectrum at an equivalent excitation energy of 11.8 MeV. However, contributions from ^{12}C originating from the frame and the foil were hardly recognizable.

Beam currents were measured by a Faraday cup. They ranged from about 0.2 to 2.0 nA, depending on the spectrometer angle. The detector efficiency for two-particle events including the tracking efficiency of the analysis software has been evaluated to be 90%. Measurements were made at three different spectrometer angle settings covering an angular range in the laboratory system from 0° to 8°. For each angle setting the data set was divided into two angular bins of equal size.

The ^{32}P spectrum was energy calibrated by matching the excitation energy of the strongest peaks to the known states at 1.15, 4.20, and 4.71 MeV [27]. We estimate the error in the excitation energy of genuinely identified peaks to be less than 25 keV, which, of course, depends on counting statistics. The hydrogen line from $^1\mathrm{H}(d,^2\mathrm{He})n$, which almost always appears in the spectra, further aids in calibrating the energy.

Figure 2 shows the excitation-energy spectrum of the ^{32}P nucleus at $\Theta_{BBS}=0°$. The measured data have been treated as described in Ref. [3]. We note that the spectra are free of any significant instrumental background or background due to random correlations. The energy resolution is 150 keV (full width at half maximum). In the present case, the resolution was not only determined by the intrinsic resolutions of the beam, the spectrometer and the detector, but also to a significant part by the target thickness. Unfortunately, it was not possible to produce a thinner target, because the pellet would have been too fragile and inhomogeneous.

The resolution still allows identification of a series of excited states in the ^{32}P daughter nucleus. Spectra have been analyzed up to an excitation energy of 7 MeV, where the density of states is still low enough to analyze clearly resolved peaks.

The $(d,^2\mathrm{He})$ cross sections $d^2\sigma/d\Omega dE$ have been integrated over the ^{2}He internal energy distribution $F(\varepsilon)$ from 0 to 1 MeV as described in Ref. [1]. Therefore, the process of the acceptance correction introduces a model-dependent scale into the determination of absolute cross sections. The analysis technique is well established for $(d,^2\mathrm{He})$ experiments, and we will use the term "absolute" for the ε-integrated cross sections.

The various yields in the spectra were determined by peak integration, where peak fitting, if necessary, was performed

with the computer program FIT [28] in manual fitting mode.

The quoted errors in cross sections reflect the counting statistics and systematic uncertainties arising from the acceptance correction procedure. Within a single angular setting, this uncertainty is about 5%, while among different angular settings, it adds to 10%.

An additional systematic error in the absolute cross sections is due to target thickness, detection efficiency, current integration, etc. It is estimated to be 10% at most.

III. DETAILED ANALYSIS

Gamow-Teller transitions from an even-even parent nucleus all lead to $J^\pi = 1^+$ final states. The distinct forward-peaked shape of the $\Delta L = 0$ angular distribution is a signature of a 1^+ excitation and is usually taken as a basis for the spin-parity assignment. For up to about 6 MeV, the presently extracted excitation energies in ^{32}P for $J^\pi = 1^+$ states have been compared with data from Ref. [27], whereas above 6 MeV they have been determined from the present data only. To further corroborate the angular momentum assignments, we performed DWBA (distorted-wave Born approximation) model calculations. Such calculations are also employed for the estimate of distortion factors, which are needed to extract B(GT$^+$) values from the cross sections (see below).

For the model calculations we used the specialized DWBA code ACCBA by Okamura [29], which treats the three-body problem in the exit channel in the adiabatic approximation, i.e., it uses deuteron and proton optical-model parameters (OMPs) in the entrance and exit channels, respectively. OMPs have been taken from Korff *et al.* [30] and from Koning *et al.* [31] for deuterons and protons, respectively.

ACCBA is a semi-microscopic code that uses an effective nucleon-nucleon (*NN*) interaction and shell-model wave functions. We took the effective *NN* interaction from Love and Franey [32], for which a parameter set at 85 MeV per nucleon has been interpolated earlier [1]. We are aware that using an effective *NN* interaction for the present $A = 2$ systems may be too simplistic as mentioned earlier, but it seems to be justifiable by the overall success in describing the data.

Nuclear wave functions have been generated by the shell-model code OXBASH [33] with the USD residual interaction of Wildenthal and Brown [34]. For the implementation into the ACCBA calculations, we took those spectroscopic amplitudes that showed the best correspondence in excitation energy and strength to those of the respective experimentally identified states, although we note that in most cases the shape of the angular distributions at forward angles does not strongly depend on the details of the wave function.

Figure 3 shows measured and calculated angular distributions of the three most strongly excited 1^+ states, together with the lowest and isolated 2^- state. The latter illustrates the difference in the angular distribution for different ΔL transfers. A general feature of all 1^+ states seems to be that the ACCBA calculations overestimate the experimental data at large angles, where the "diffraction" structure of the calculated angular distributions is much less pronounced experimentally. To describe the 2^- transition in the shell-model, we assume the *p* shell to be closed so that the observed 2^- level must be a $1\,\hbar\omega$ transition into the *pf* shell. The most probable mode is a simple $(\pi^{-1}1d_{5/2} - \nu 1f_{7/2})$ configuration. At the lowest momentum transfer, the calculation underestimates the cross section. However overall, the calculation fits the experimental data reasonably well, indicating that the model gives a good description of the reaction.

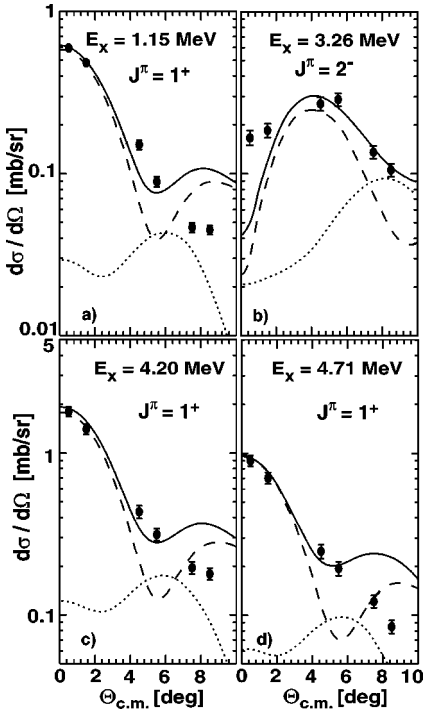

FIG. 3. Experimental ^{32}S$(d,{}^2\mathrm{He})^{32}$P, differential cross sections for the prominent 1^+ states at (a) 1.15 MeV, (c) 4.20 MeV and (d) 4.71 MeV and the 2^- state at (b) 3.26 MeV. The solid lines represent the full ACCBA calculations ($\Delta L = 0$ and $\Delta L = 2$); the dashed and dotted lines describe the central part and tensor part, repectively.

For the 1^+ states, we performed a cross-check using the semi-microscopic DWBA code DW81 [35], which has no special treatment of the outgoing ^{2}He. The exit channel distortion is described by deuteron OMPs. The calculated angular distributions show, besides a scaling difference, no significant deviations from the ACCBA results.

Further 1^+ states are known from Ref. [27] to be at 0.0, 2.23, 2.74, 3.79, 4.55, and 5.67 MeV. These states are also excited by the $(d,{}^2\mathrm{He})$, reaction, although weakly, and it is therefore difficult to separate them from neighboring states (cf. the labeling in Fig. 2). For instance, the state at 4.55 MeV disappears under the two states at 4.20 and 4.71 MeV, and the 1^+ state at 2.74 MeV may be accompanied by the weaker 3^+ state at 3.03 MeV.

Above 5 MeV, three distinct levels can be resolved. The states found at 5.67 and 7.01 MeV are well described by a $\Delta L = 0$ angular distribution, while the angular distribution of the 6.51 MeV level indicates the presence of contaminations from higher multipoles, i.e., $(1,2)^-$ and $(2,3)^+$ contributions from neighboring unresolved states. For weakly excited

states, especially those which do not show a pure $\Delta L=0$ angular shape, the extracted B(GT) strength parameters have usually been marked with an additional 30% error in Table II.

The transition to the 1^+ ground state in ^{32}P is *l*-forbidden and will be subject of a separate discussion below.

IV. B(GT) STRENGTH ANALYSIS

A. Calibration of B(GT$^+$) strength

In this section we aim at calibrating the $(d,{}^2\mathrm{He})$ probe for the extraction of Gamow-Teller strength in the β^+ direction. In order to relate the cross sections to B(GT) values, we exploit isospin symmetry and compare the $^{32}\mathrm{S}(d,{}^2\mathrm{He})^{32}\mathrm{P}$ cross sections to analog B(GT$^-$) values which are known with good precision from $^{32}\mathrm{S}(p,n)^{32}\mathrm{Cl}$ measurements [15].

Cross sections from $(d,{}^2\mathrm{He})$ experiments can be connected to B(GT$^+$) values through a simple relationship in close analogy to the (n,p) case [1,36,37]

$$\left(\frac{d\sigma(q=0)}{d\Omega}\right)_{(d,{}^2\mathrm{He})} = C\left[\left(\frac{\mu}{\pi\hbar^2}\right)^2\frac{k_f}{k_i}N_D J_{\sigma\tau}^2 B(GT^+)\right]. \quad (1)$$

The scaling factor C is inserted, because the $(d,{}^2\mathrm{He})$ response additionally scales with the distribution of the $d \xrightarrow{\mathrm{GT}^-} {}^2\mathrm{He}$ transition strength, whose detection is limited by the experimental setup [3,38].

The cross sections are first extrapolated to zero momentum transfer $(q=0)$ using the DWBA calculations:

$$\frac{d\sigma(q=0)}{d\Omega} = \left(\frac{\sigma(q=0)}{\sigma(\Theta,q)}\right)_{\mathrm{DWBA}}\left(\frac{d\sigma(\Theta,q)}{d\Omega}\right)_{\mathrm{exp}}. \quad (2)$$

Then, distortion factors N_D are computed (using the ACCBA code) by the ratio between distorted-wave (DW) and plane-wave (PW) cross sections:

$$N_D = \frac{\sigma_{\mathrm{DW}}(q=0)}{\sigma_{\mathrm{PW}}(q=0)}. \quad (3)$$

The PW cross sections are obtained by setting all potential strengths to zero.[1] For the $^{32}\mathrm{S}(d,{}^2\mathrm{He})^{32}\mathrm{P}$ reaction the calculation yielded $N_D=0.099\pm0.006$. The volume integral of the effective central $\boldsymbol{\sigma\tau}$ interaction at $E/A=85$ MeV is taken as $|J_{\sigma\tau}|=165$ MeV fm^3 [40].

Following this, individual scaling factors, C_i, for each level are being determined from the experimental cross sections and from the reference B(GT$^-$) values of the $^{32}\mathrm{S}(p,n)$ reaction [15]. Here, only strongly excited states have been taken into account, because of the larger uncertainties involved for weak states. For this, we chose the limit to be B(GT$^-$)$\gtrsim$0.070. The various levels are listed in Table I. The scaling factors for each of the considered levels give rather consistent values, except for the state at $E_x=4.71$ MeV, where there is surprisingly almost a factor of 2 difference

TABLE I. GT strength from $^{32}\mathrm{S}(p,n)$ [15], cross sections from $(d,{}^2\mathrm{He})$, and individual scaling factors C_i from the present experiment. The quoted errors are statistical. Only the most strongly excited states (B(GT$^-$)$\gtrsim$0.07) are taken into account for the calibration.

Reference data [15]		Present data		
E_x [MeV]	B(GT$^-$)	E_x [MeV]	$d\sigma(q=0)/d\Omega$ [mb/sr]	C_i
1.15	0.344±0.004	1.15	0.659±0.038	0.343
4.06	1.005±0.006	4.20	1.877±0.100	0.337
4.58	0.310±0.004	4.71	1.050±0.059	0.613[a]
5.41	0.087±0.002	5.67	0.181±0.013	0.378
6.65	0.068±0.023	7.01	0.164±0.013	0.440

[a]State not taken into account for calibration; see the text.

Once the individual scaling factors have been determined, they are combined to an overall calibration factor by cross section weighted averaging. However, we exclude the aforementioned state at $E_x=4.71$ MeV, as this state requires a separate discussion, which will be performed in the following section in the light of the results from the (p,p'), and (e,e') probes. Combined with the previous measurements on ^{12}C and ^{24}Mg from Ref. [1], together with further data[2] on ^{12}C, the value obtained is:

$$C = 0.320 \pm 0.027.$$

In Table II, this factor is applied to all transitions in order to determine their individual GT$^+$ strengths and the total summed strength.

To give an overview of all *p* and *sd* shell nuclei we surveyed so far, we plotted in Fig. 4 the reduced $(d,{}^2\mathrm{He})$ cross section for each strong transition in ^{12}C, ^{24}Mg (both taken from from Ref. [1]) and ^{32}S versus the reference B(GT$^-$) values from Refs. [15,16].

B. Comparison with (p,n), (e,e') and (p,p') reactions and a shell-model calculation

In this section we compare transitions from the ^{32}S ground state to the various $T=1$ isobaric analog states in ^{32}P, ^{32}S, and ^{32}Cl which are excited through $(d,{}^2\mathrm{He})$, (p,p') or (e,e'), and (p,n) reactions, respectively.

[1]We note that for calculating N_D in Ref. [1], the PW calculations were performed without the Coulomb potential being turned off. After a modification of the ACCBA code, it has now become possible to switch off the Coulomb potential for the purpose of calculating the projectile/ejectile distortion. For the nuclei considered so far (^{12}C, ^{24}Mg), the effect is a slight decrease of N_D (−2% for ^{12}C and −13% for ^{24}Mg), requiring an increased value for the scaling factor *C*.

[2]We note that in each experiment, a measurement on a carbon target is taken as a reference. Over many of these measurements the experimental zero-degree cross section has scattered between 1.7 and 2.1 mb/sr giving a mean value of 1.9±0.2 mb/sr, which is the value adopted in the present analysis. This variance is also a good measure of the systematic error.

TABLE II. Comparison of B(GT$^+$), B(GT$^-$), B(M1), and B(σ) strengths extracted from the $(d,^2\mathrm{He})$ (present data), (p,n), (e,e'), and (p,n) reactions on ^{32}S, respectively (from Refs. [15,20,21,39]). Excitation energies in ^{32}S are taken from the (p,p') measurement. Energy deviations between (p,p') and (e,e') are smaller than 40 keV. B(M1) and B(σ) have been transformed to B(GT) units (see the text). The given uncertainties are sums of statistical and systematic errors.

E_x [MeV]	B(GT$^+$)	E_x [MeV]	B(GT$^-$)	E_x [MeV]	B(M1)	B(σ)
0	$(3.8\pm1.9)10^{-4}$[a]	0	0.014±0.010	6.98[b]	0.002±0.001	0.008±0.004
1.15	0.369±0.052	1.15	0.344±0.045	8.13	0.329±0.034	0.552±0.073
2.23[c]	0.039±0.016			9.28[b]		0.019±0.004
2.74	0.066±0.027	2.79	0.071±0.011	9.66	0.140±0.023	0.064±0.024
3.79[c]	0.121±0.046	3.73	0.025±0.009			
4.20	1.060±0.145	4.06	1.005±0.127	11.13	0.795±0.057	1.544±0.295
4.71	0.594±0.083	4.58	0.310±0.041	11.63	0.393±0.035	0.900±0.132
5.67	0.103±0.039	5.41	0.087±0.012	12.56		0.124±0.011
6.31[c]	0.040±0.016	6.06	0.033±0.006	13.23[b]		0.015±0.004
6.51[c]	0.124±0.048	6.29	0.021±0.009	13.77[b]		0.011±0.004
7.01	0.093±0.015	6.65	0.068±0.031	13.90		0.091±0.011

[a]Deduced from calculations, systematical error cannot be estimated.
[b]Denotes states which have been given an isospin $T=0$ assignment by Crawley *et al.* [21] but have also been seen in (e,e').
[c]Denotes peaks which carry additional strength from higher multipole contributions and which have been given an extra 30% error as described in the text.

Figure 5 visualizes the similarity of the $(d,^2\mathrm{He})$ spectrum to the spectra of each considered reaction. Further, we plotted the present B(GT$^+$) values versus B(GT$^-$), $B_{pp'}(\sigma)$, and $B_{ee'}$(M1) in parts (a), (b), and (c).

Table II gives, apart from the B(GT$^+$) strength values, also the strength parameters deduced from each of the other reactions. For a more convenient comparison, the B(M1) and B(σ) values may be transformed to B(GT) units using the relation

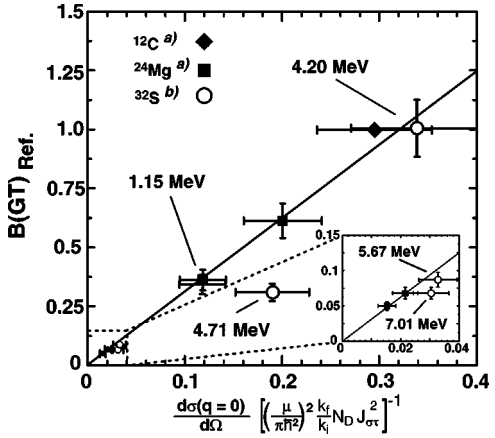

FIG. 4. The inverse of the slope of the linear fit represents the calibration factor (see the text). Numerical excitation energy values are given only for the levels of ^{32}P from the present analysis. In the inset, the region of small B(GT) values is plotted separately. The errors bars correspond to a 20% error of the $(d,^2\mathrm{He})$ cross sections and a 12% error of the B(GT$^-$) based on (p,n) data [15,16]. The error of the reference B(GT) value from the ^{12}B β-decay is too small to be displayed.

$$\mathrm{B}(\sigma) = \frac{3(\mu_p - \mu_n)^2}{8\pi}\mathrm{B(GT)} = 2.643\mu_N^2\mathrm{B(GT)}. \qquad (4)$$

1. The case of (p,n)

As already mentioned, the comparison of the $(d,^2\mathrm{He})$ with the (p,n) data is the basis of the B(GT$^+$) extraction in the present case and yields a single scaling factor between the normalized $(d,^2\mathrm{He})$ cross section and the B(GT$^-$) values. A marked exception from this simple relationship is the rather strongly excited 1^+ state at 4.71 MeV, which, in the (p,n) case, seems to be suppressed by as much as ≈40% [see the lower panel of Fig. 5(a)]. Since an error in the (p,n) time-of-flight measurement [15] is highly unlikely, one may speculate if this suppression could be an indication for a mirror symmetry breaking in the nuclear structure. Although of interest in the context of isospin symmetry breaking studies [14], such a large value is, however, rather unexpected. It may therefore be instructive to further investigate the structure of this state by examining its behavior when excited by the other probes.

2. The case of (p,p')

Figure 5(b) shows the comparison between B(GT$^+$) and B(σ) strength from the (p,p') experiment by Crawley *et al.* [21]. Here, we observe that the state at 4.71 MeV has the same relative strength as all the other states when compared to the $(d,^2\mathrm{He})$ reaction (cf. also Table II). However, the slope of the linear fit is about 55% higher than the expected value of $2.643\mu_N^2$, which may be due to an erroneous evaluation of the (p,p') unit cross section used for the conversion of ex-

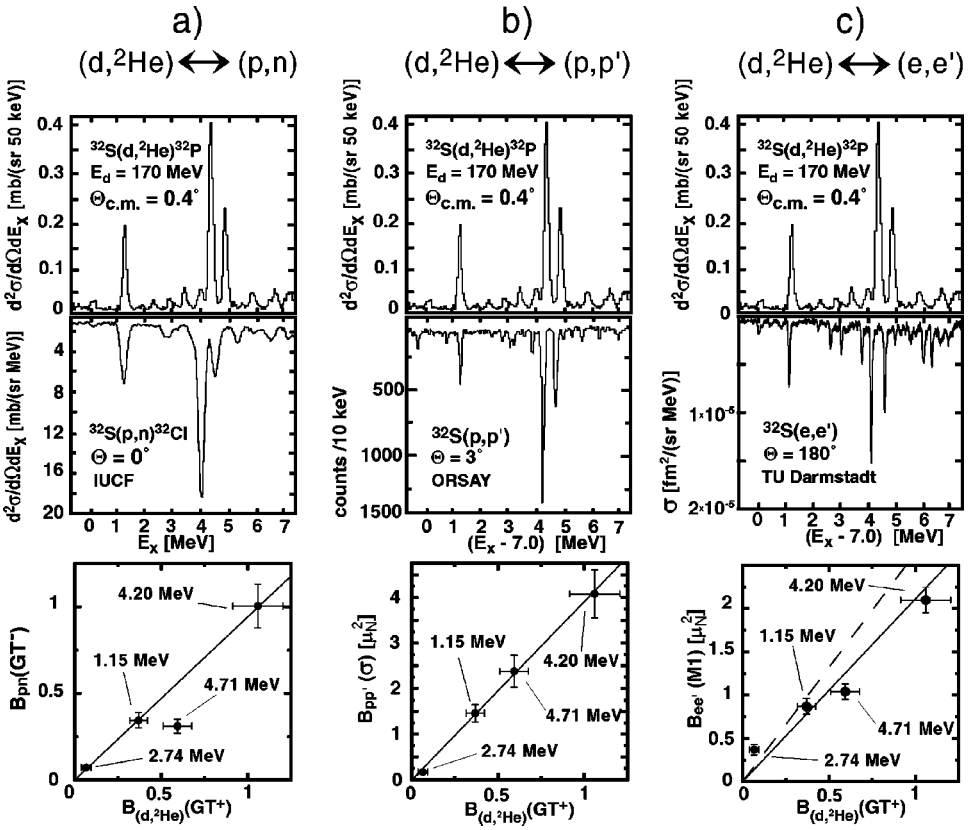

FIG. 5. Comparison of $(d,{}^2\mathrm{He})$ spectra with those from various mirror reactions. The (e,e') and (p,p') spectra are offset by 7.0 MeV. In the graphs at the bottom are plotted the $B(GT^+)$ values vs the corresponding $B(GT^-)$, $B(\sigma)$, and B(M1) values. The dashed line shown in the bottom panel of part (c) indicates the expected proportionality with a slope of $2.643\mu_N^2$ (see the text).

perimental cross sections to transition strengths. Such a discrepancy has already been noted in Refs. [20,41].

3. The case of (e,e')

The comparison with (e,e') data from Ref. [20] as displayed in part (c) of Fig. 5 shows again a linear relation between $B(GT^+)$ and B(M1) transition strengths with no marked exception. However, the extracted slope of the regression line appears to be about 20% below the expected value of $2.643\mu_N^2$. On the other hand, a line with a slope at the correct value of $2.643\mu_N^2$ places the two strongest states at 4.20 and 4.71 MeV significantly below the line, leading to the interpretation that both of these states contain significant orbital contributions and/or meson-exchange currents, which in (e,e') scattering interfere with the spin excitation part [41,42].

4. Conclusion

From the previous discussions we conclude that apart from the 4.71 MeV state, whose discrepancy with the other probes cannot be resolved, all 1^+ states observed in the $(d,{}^2\mathrm{He})$ reaction show the expected behavior when excited by the other probes. With the extraction of absolute $B(GT^+)$ values, a direct comparison with the results of the shell-model calculations can now be performed. Such a comparison is shown in Fig. 6, where the USD residual interaction [34] was employed. Apart from the usual quenching factor, there is good correspondence between the experimental and theoretical strength distributions.

Combining all results, one can now link the analog states in the $A=32$, $T=1$ isospin triplet. Figure 7 shows the level schemes of the three isobars ^{32}P, ^{32}S, and ^{32}Cl. Note that for (e,e') and (p,p') data, excitation energies in the ^{32}S nucleus are offset by 7.0 MeV. All strong, and even most of the weak 1^+ states can be identified in the isospin triplet up to 7 MeV

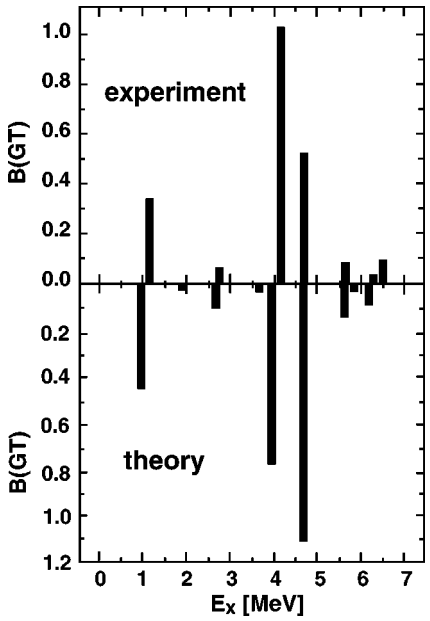

FIG. 6. Comparison of experimental and theoretical $B(GT^+)$ strengths in ^{32}P. The shell-model calculation was performed using the USD interaction of Wildenthal and Brown [34].

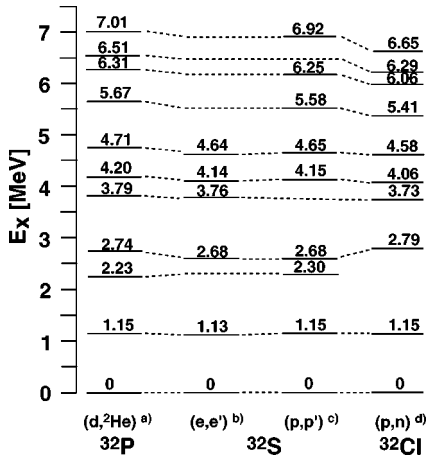

FIG. 7. Analog $J^{\pi}=1^{+}$ states in the $A=32$ triad.

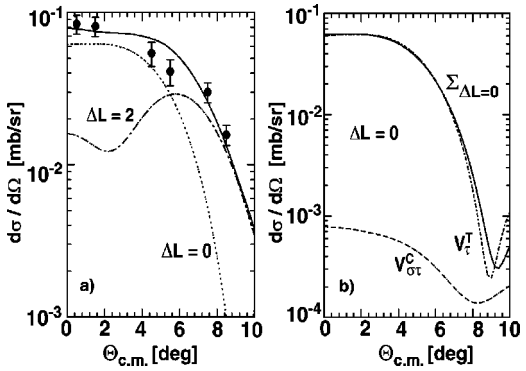

FIG. 8. Experimental ^{32}S$(d,^{2}$He$)^{32}$P differential cross sections for the two states near 0 MeV. The $\Delta L=0$ calculation is represented by the dotted line, the $\Delta L=2$ calculation by the dashed line. The curves have been scaled and added so that the sum (solid line) gives a fit to the data (left panel). The $\Delta L=0$ contribution is separated into the central $V_{\sigma\tau}$ part and tensor V_{τ}^{T} part (right panel).

excitation energy. The systematically appearing slight differences in excitation energies along the isobars are attributed to Coulomb displacement effects [43].

C. *l*-forbidden ground state transition

In the simple shell-model, the transition from ^{32}S(0^{+}) to the ^{32}P or ^{32}Cl(1^{+}) ground state involves a change from an $s_{1/2}$ to a $d_{3/2}$ orbit. Such a transition cannot be mediated by the GT operator and is therefore referred to as *l*-forbidden [44,45]. Ground state correlations, however, weaken this argument and any sizable excitation of the ^{32}P(1^{+}) ground state through the $(d,^{2}$He) reaction could be referred to as an indicator for such correlations. (We note that another possible cause for such a transition has been discussed in terms of "pseudospin symmetry," [46] which describes the quasidegeneracy of the $2s_{1/2}$ and $1d_{3/2}$ shells in deformed nuclei; however, a discussion along these lines cannot be entertained in the present case of ^{32}S.) On the other hand, the log ft value of the decay of ^{32}P to the ground state of ^{32}S(BR $=100\%$) is known to be sizable (log $ft=7.9$), which would point to a rather reduced GT transition strength. Yet, Anderson *et al.* [15] deduced from their (p,n) data the mirror GT transition strength to the ^{32}Cl(1^{+}) ground state to be $B(GT^{-})=0.014\pm0.01$. This value would transform into an ft value (log $ft=5.9$), which is more than a factor of 6 smaller than presently accepted for the ^{32}Cl decay (log $ft=6.7$).

The $(d,^{2}$He) spectrum for ^{32}S shows in the region of the ^{32}P ground state a clear indication for the presence of a weak transition (cf. Fig. 2). Unfortunately, the difficulty in analyzing this transition is not only governed by low counting statistics, but rather due to the fact that in ^{32}P there is a low-lying 2^{+} state located only 79 MeV above the ground state. Disentangling both transitions was not possible with the present resolution and therefore both peaks had to be treated together.

Figure 8 shows the angular distribution of the g.s. +0.079 MeV structure together with a detailed model analysis for both states. In describing the analysis, it is instructive to recall that a $0^{+}\rightarrow1^{+}$ spin-flip transition at $q=0$ usually occurs through a strong $\Delta L=0$ component governed by the $V_{\sigma\tau}$ part of the effective interaction, and a generally weak $\Delta L=2$ component governed by the tensor part V_{τ}^{T}. The ratio of the contributions at $\Theta=0°$ is usually about 20:1 (cf. Fig. 3 and Ref. [1]). For the present analysis, we performed separate $\Delta L=0$ and $\Delta L=2$ calculations and assumed that the transition to the 0.079 MeV (2^{+}) state proceeds through a $\Delta L=2$ transition of the same angular shape as the $\Delta L=2$ transition to the ground state. The two curves are then added to fit the experimental data.

For the DWBA calculation of the ground state transition, a ground state shell-model wave function was generated using the USD residual interaction of Wildenthal and Brown [34]. The reaction calculation then reveals that the transition to the ^{32}P ground state is not governed by the central $V_{\sigma\tau}$ term, but rather dominated by the tensor force, as was already noticed in Ref. [45]. The zero-degree charge-exchange cross section for a transition from the ^{32}S ground state to the ground state of its isobar is, thus, one of the rare cases where a $\Delta L=0,0^{+}\rightarrow1^{+}$ transition is not governed by the GT operator! To illustrate this situation, the right-hand side of Fig. 8 shows the two contributions to the $\Delta L=0$ transition separately together with the sum of both. At zero degree, the tensor component is about 2 orders of magnitude enhanced over its central $V_{\sigma\tau}$ counterpart. One may also note that the shape of the angular distribution for such a case is much less steep than what one would usually expect for a pure GT transition.

As already indicated, the $\Delta L=0$ and $\Delta L=2$ contributions were then adjusted to fit the experimental angular distribution in Fig. 8(a). The extracted GT ground state transition strength resulted in $B(GT^{+})=(3.8\pm1.9)\times10^{-4}$, which transforms to a β^{-} decay log ft value of log $ft=7.5^{+0.5}_{-0.6}$ in agreement with the presently accepted value of log $ft=7.9$ for the decay of ^{32}P.

V. CONCLUSIONS

Differential cross sections for transitions from ^{32}S in the β^+ direction have been measured by the $(d,{}^2\mathrm{He})$ reaction. The energy resolution of 150 keV and the angular distributions allowed identification of various 1^+ states in the daughter nucleus ^{32}P. Due to the nature of the reaction, these transitions are of Gamow-Teller type. Angular distributions of cross sections have been analyzed using phenomenological and semi-microscopic DW model calculations.

The zero-degree cross sections have been compared to known Gamow-Teller mirror transition strengths by exploiting isospin symmetry, and an overall scaling factor, which relates the zero-degree cross sections to $\mathrm{B(GT^+)}$ values, has been extracted.

A further comparison with (p,p') and (e,e') data have lead to a level scheme containing the $1^+(T=1)$ levels of the $A=32$ isospin triad.

The issue of the *l*-forbidden ground state transition has been addressed. It was found that the transition is largely governed by the tensor part of the effective interaction. A small contribution from the GT transition operator is in accordance with the beta decay log *ft* value.

ACKNOWLEDGMENTS

We wish to thank S. Brandenburg and the KVI accelerator staff. We thank H. Okamura for providing the ACCBA code. We are particularly grateful to B. D. Anderson and F. Hofmann, who have provided us with the $^{32}\mathrm{S}(p,n)$ and $^{32}\mathrm{S}(e,e')$ data sets, and C. Djalali for granting us permission to show the $^{32}\mathrm{S}(p,p')$ data. We thank H. Baumeister (IKP Münster) for making the target. This work was performed with support from the Land Nordrhein-Westfalen and the EU under Contract No. TMR-LSF ERBIMGECT980125. It was further performed as part of the research program of the Stichting FOM with financial support from the Nederlandse Organisatie voor Wetenschappelijk Onderzoek and as part of the research program of the Fund for Scientific Research-Flandres.

[1] S. Rakers *et al.*, Phys. Rev. C **65**, 044323 (2002).
[2] C. Bäumer *et al.*, Phys. Rev. C **68**, 031303 (2003).
[3] S. Rakers *et al.*, Nucl. Instrum. Methods Phys. Res. A **481**, 253 (2002).
[4] M. Hagemann *et al.*, Phys. Lett. B **579**, 251 (2004).
[5] R. Helmer, Can. J. Phys. **65**, 588 (1987).
[6] G. M. Fuller, W. A. Fowler, and J. Newman, Astrophys. J. **293**, 1 (1985); Astrophys. J., Suppl. **48**, 279 (1982); Astrophys. J. **252**, 715 (1982); Astrophys. J., Suppl. **42**, 477 (1980).
[7] K. Langanke and G. Martínez-Pinedo, Rev. Mod. Phys. **75**, 819 (2003).
[8] S. Nakayama *et al.*, Phys. Rev. C **60**, 047303 (1999).
[9] N. Anantaraman *et al.*, Phys. Rev. C **44**, 398 (1991).
[10] T. Ichihara *et al.*, Phys. Lett. B **323**, 278 (1994).
[11] B. M. Sherrill *et al.*, Nucl. Instrum. Methods Phys. Res. A **432**, 299 (1999).
[12] I. Daito *et al.*, Phys. Lett. B **418**, 27 (1998).
[13] R. E. McDonald *et al.*, Phys. Rev. C **10**, 333 (1974).
[14] N. A. Smirnova *et al.*, Nucl. Phys. **A714**, 441 (2003), and references therein.
[15] B. D. Anderson *et al.*, Phys. Rev. C **36**, 2195 (1987).
[16] B. D. Anderson *et al.*, Phys. Rev. C **43**, 50 (1991); (private communication).
[17] J. Rapaport *et al.*, Phys. Rev. C **24**, 335 (1981).
[18] H. Akimune *et al.*, Nucl. Phys. **A569**, 245c (1994).
[19] Y. Fujita *et al.*, Phys. Lett. B **365**, 29 (1996).
[20] F. Hofmann *et al.*, Phys. Rev. C **65**, 024311 (2002).
[21] G. M. Crawley *et al.*, Phys. Rev. C **39**, 311 (1989).
[22] H. J. Wörtche, Nucl. Phys. **A687**, 321c (2001).
[23] M. Hagemann *et al.*, Nucl. Instrum. Methods Phys. Res. A **437**, 459 (1999).
[24] B. A. M. Krüsemann *et al.*, IEEE Trans. Nucl. Sci. **47**, 2741 (2001).
[25] A. M. van den Berg, Nucl. Instrum. Methods Phys. Res. B **99**, 637 (1995).
[26] A. M. van den Berg *et al.*, KVI Annual Report, 1998, p. 55.
[27] P. M. Endt, Nucl. Phys. **A521**, 1 (1990).
[28] S. Strauch and F. Neumeyer, computer program FIT, TU Darmstadt, Germany, 1995.
[29] H. Okamura, Phys. Rev. C **60**, 064602 (1999).
[30] A. Korff *et al.* (unpublished).
[31] A. J. Koning and J. P. Delaroche, Nucl. Phys. **A713**, 231 (2002).
[32] M. A. Franey and W. G. Love, Phys. Rev. C **31**, 488 (1985).
[33] B. A. Brown *et al.*, computer program OXBASH (unpublished).
[34] B. H. Wildenthal, Prog. Nucl. Phys. **11**, 5 (1984); B. A. Brown and B. H. Wildenthal, Phys. Rev. C **27**, 1296 (1983).
[35] R. Schaeffer and J. Raynal, program DWBA70, (unpublished); extended version DW81 by J. R. Comfort (unpublished).
[36] T. N. Taddeucci *et al.*, Nucl. Phys. **A469**, 125 (1987).
[37] C. D. Goodman *et al.*, Phys. Rev. Lett. **44**, 1755 (1980).
[38] H. Okamura *et al.*, Nucl. Instrum. Methods Phys. Res. A **406**, 78 (1998).
[39] B. Reitz, Diploma thesis, TU Darmstadt, 1996.
[40] W. G. Love and M. A. Franey, Phys. Rev. C **24**, 1073 (1981).
[41] A. Richter *et al.*, Phys. Rev. Lett. **65**, 2519 (1990).
[42] Y. Fujita *et al.*, Phys. Rev. C **62**, 044314 (2000).
[43] C. Jeanperrin *et al.*, Nucl. Phys. **A503**, 77 (1989).
[44] B. Reitz *et al.*, Phys. Rev. Lett. **82**, 291 (1999).
[45] P. von Neumann-Cosel, Prog. Part. Nucl. Phys. **44**, 49 (2000).
[46] J. N. Ginocchio, Phys. Rev. C **59**, 2487 (1999).